SCIPEDIA

Solving the Sine-Gordon Equation: A Novel Numerical Approach Using Cubic B-Splines and the Method of Lines

Irsa Ashraf[1], Muhammad Yaseeen[1,*], Salma Trabelsi[2] and Marwa Balti[2,*]

[1] Department of Mathematics, University of Sargodha, Sargodha, 40100, Pakistan

[2] Department of Mathematics and Statistics, College of Science, King Faisal University, Al Ahsa, 31982, Saudi Arabia

INFORMATION

Keywords:
Sine-Gordon equation
method of lines
cubic B-Spline interpolation
stability analysis
convergence analysis
fourth-order Runge-Kutta method
numerical error

DOI: 10.23967/j.rimni.2025.10.72566

SCIPEDIA
Revista Internacional de Métodos Numéricos para Cálculo y Diseño en Ingeniería
RIMNI

Solving the Sine-Gordon Equation: A Novel Numerical Approach Using Cubic B-Splines and the Method of Lines

Irsa Ashraf[1], **Muhammad Yaseeen**[1,*], **Salma Trabelsi**[2] **and Marwa Balti**[2,*]

[1]Department of Mathematics, University of Sargodha, Sargodha, 40100, Pakistan

[2]Department of Mathematics and Statistics, College of Science, King Faisal University, Al Ahsa, 31982, Saudi Arabia

ABSTRACT

This work explores a numerical approach to solving the sine-Gordon equation using the method of lines combined with cubic B-spline interpolation. The sine-Gordon equation, a nonlinear partial differential equation, arises in various fields of physics and engineering, describing phenomena such as solitons in non-linear optics and magnetic flux lines in superconductors. In our approach the method of lines is used to discretize the spatial derivatives, thereby converting the partial differential equation into a system of ordinary differential equations. These ordinary differential equations are then solved numerically using standard techniques, specifically the Runge-Kutta method of order 4. Cubic B-spline interpolation is employed to approximate the spatial derivative, ensuring efficient and precise computation of the solution. A comprehensive stability analysis reveals that our scheme requires the time step condition $\Delta t \lessapprox 1.53\, h$ for numerical stability. Theoretical convergence analysis demonstrates that the method achieves $O(h^2)$ spatial convergence and $O(\Delta t^4)$ temporal convergence, resulting in an overall error bound of $O(h^2 + \Delta t^4)$. These theoretical predictions are strongly supported by numerical experiments, where empirical convergence rates closely match the theoretical values. To validate the numerical scheme, the results are compared with existing solutions. Our findings demonstrate the accuracy and computational efficiency of the proposed method, highlighting its potential as a valuable tool for studying the dynamics and behavior of systems governed by the sine-Gordon equation.

OPEN ACCESS

Received: 29/08/2025

Accepted: 05/11/2025

Published: 23/01/2026

DOI
10.23967/j.rimni.2025.10.72566

Keywords:
Sine-Gordon equation
method of lines
cubic B-Spline interpolation
stability analysis
convergence analysis
fourth-order Runge-Kutta method
numerical error

1 Introduction

The sine-Gordon equation is a non-linear partial differential equation (PDE) that is found in various physical and engineering applications, such as non-linear optics, superconductivity, and the study of solitons. This equation is known for its intricate mathematical structure and its ability to describe a wide range of phenomena, including soliton solutions and chaotic behavior. Consequently, accurately and efficiently solving the sine-Gordon equation is of great interest to both theorists and practitioners.

*Correspondence: Muhammad Yaseeen, Marwa Balti (yaseen.yaqoob@uos.edu.pk, mbalti@kfu.edu.sa).

Numerical methods are essential in studying the sine-Gordon equation due to the difficulty of obtaining analytical solutions for most practical problems. The method of lines (MOL) has become popular for its flexibility and effectiveness, as it transforms the PDEs into a system of ordinary differential equations (ODEs) by discretizing the spatial derivatives. These ODEs can then be solved using standard numerical techniques. The choice of spatial discretization method significantly impacts the accuracy and efficiency of the MOL.

In this study, we present a new numerical approach for solving the sine-Gordon equation that combines the method of lines with cubic B-spline interpolation. Cubic B-splines are known for their smoothness and accuracy in approximating functions and their derivatives. By using cubic B-splines for spatial discretization, we aim to improve the precision and computational efficiency of the numerical solution.

We consider the following one-dimensional, non-linear, time dependent sine-Gordon equation:

$$\frac{\partial^2\varphi}{\partial t^2} = \frac{\partial^2\varphi}{\partial s^2} - \sin\varphi, \quad s \in [\beta_1, \beta_2], \quad t > 0, \tag{1}$$

having IC's,

$$\begin{cases} \varphi(s,0) = h_1(s), \\ \frac{\partial\varphi}{\partial t}(s,0) = h_2(s), \end{cases} \tag{2}$$

and Dirichlet BC's,

$$\begin{cases} \varphi(\beta_1,t) = f_1(t), \\ \varphi(\beta_2,t) = f_2(t), \end{cases} \quad t \geq 0, \tag{3}$$

The sine-Gordon equation is given by Edmound Bour in the course of study of surfaces of constant negative curvature as the Gauss-Codazzi equation for the surface of constant Gaussian curvature. Dehghan and Shokri [1] presented a meshless numerical method based on radial basis functions to solve the non-linear Klein-Gordon equation. This approach is an effective and accurate alternative to traditional mesh-based techniques for this class of problems. Jokela et al. [2] investigated the sine-Gordon model in the context of a time-like boundary field theory. Their research established a theoretical connection between this quantum field theory and the statistical mechanics of a two-component Coulomb plasma. Novkoski et al. [3] developed a numerical direct scattering scheme to investigate the periodic sine-Gordon equation, providing accurate insights into its wave behavior and periodic structures. Tamsir et al. [4] introduced a differential quadrature method based on cubic unified and extended trigonometric B-splines which demonstrated enhanced accuracy and stability in solving the sine-Gordon equations. Chu et al. [5] demonstrated an advanced cubic B-spline scheme to find the accurate numerical results of the non-linear sine-Gordon equations across multiple dimensions. Wang et al. [6] introduced a novel cubic B-spline collocation approach enhanced with an adaptive mechanism to solve the sine-Gordon equation. Veeresha et al. [7] proposed two efficient numerical techniques to address the nonlinear sinne-Gordon equations, demonstrating improved computational performance and convergence. Li and Chen [8] established the stability and effectiveness of a novel method for solving coupled sine-Gordon equations on unbounded domains, addressing complex wave interactions. Mohebbi and Dehghan [9] give a higher order solution of the one-dimensional sine-Gordon equation using compact fourth order finite difference approximation with a fourth order A-stable DIRKIN method. Uddin et al. [10] proposed a meshfree method of lines using radial basis functions to solve the nonlinear sine-Gordon equation. Savovic et al. [11] applied a physics-informed neural network combined with two finite difference methods to obtain numerical solutions of the sine-Gordon equation. Wei [12] utilized a discrete singular convolution algorithm for integrating (1). Batiha et al. [13] proposed a variational iteration method for finding the general analytical solution of the sine-Gordon equation. Zheng [14] provided a mathematical solution for the sine-Gordon equation bounded across the real axis. Forth order rational approximation to the matrix exponential form in a three time level recurrence relation for the mathematical solution of sine-Gordon equation is presented by Bratsos [15]. By collocation points and approximating the solution by radial basis function Dehghan and Shokri [16] solved the sine-Gordon equation. The boundary integral equation method is used by Dehghan and Mirzaei [17]. By using the spline function approximation two implicit finite difference schemes are proposed by Rashidinia and Mohammadi [18]. Without solving the huge-scale linear system of equations a meshless technique by using a multi-quadric quasi interpolation is proposed by Ma et al. [19]. Jiang and Wang [20] developed a meshless method based on multiquadric quasi-interpolation to solve the sine-Gordon equation.

Khan et al. [21] applied the homotopy analysis natural transform to solve nonlinear partial differential equations. This method is an effective analytical technique that combines the natural transform with homotopy analysis. Yaseen and Samraiz [22] proposed a modified new iterative method for solving both linear and nonlinear Klein-Gordon equation. Their approach provided a simple and efficient computational tool that does not require linearization or perturbation. Mittal and Bhatia [23] developed a numerical scheme based on a modified cubic B-spline collocation method for the nonlinear sine-Gordon equation. This method handled the propagation of solitary waves accurately. Uddin et al. presented a meshfree approach using radial basis functions for the numerical solution of the nonlinear sine-Gordon equation without using a structured mesh, offering flexibility for complex geometries. Uddin et al. [24] presented a meshless method of lines for the numerical solution of the nonlinear sine-Gordon equation. Raslan et al. [25] conducted a comparative study, applying the standard finite difference method and non-standard finite difference method to the sine-Gordon equation. Vivas-Cortez et al. [26] presented an extended cubic B-spline method to find the solution of the generalized nonlinear time-fractional Klein-Gordon equation gives accurate numerical results. Their approach proved the modeling of complex fractional dynamics in mathematical physics. Deresse and Dufera [27] applied physics-informed neural networks to solve the 2D nonlinear sine-Gordon equation. Their deep learning approach demonstrated the capability of PINNs to handle the complexities of higher-dimensional problems. Deresse and Dufera [28] explored the use of a deep learning framework for the generalized nonlinear sine-Gordon equation.

In this paper, we focus on the numerical solution of the one-dimensional non-linear sine-Gordon equation using the method of lines combined with cubic B-spline interpolation. We choose various examples of the sine-Gordon equation to show the accuracy of our method, showing that the results obtained are superior to those obtained by different methods in past years.

The structure of the remaining paper is as follows: Section 2 presents the derivation of a computational technique using the method of lines based on the cubic B-spline function with a new approximation for the sine-Gordon equation. Section 3 introduces the stability analysis and Section 4 provides the convergence analysis of the proposed scheme. In Section 5, we compare our numerical results with several other numerical results found in the literature. Finally, the paper concludes with a summary of our proposed scheme.

2 The Derivation of the Scheme

This section details the derivation of our numerical scheem, which is based on a specifice formulation of the cubic B-spline within the method of lines The main aspect of our study is the direct interpolation of the solution function $\phi(s,t)$ using cubic B-splines, which allows for a consistent and high-order discretization of both the spatial derivative and the non-linear term. This leads toa computationally efficient system of ordinary differential equations.

Let $\Delta t = \frac{t}{T}$ and $h = \frac{\beta_2-\beta_1}{M}$ with T and M being positive integers. We divide the domain $\beta_1 \leq w \leq \beta_2$ into M equivalent subintervals $[w_j, w_{j+1}]$ for $j = 0, 1, 2, \ldots, M+1$ with $\beta_1 = w_0 < w_1 < \ldots < w_{M-1} < w_M < w_{M+1} = \beta_2$. Spatial derivatives are dicretize using cubic B-splines. By considering the cubic B-spline basis functions, $B_j^3(w)$ defined as:

$$B_j^3(w) = \frac{1}{6h^3}\begin{cases} (w-w_j)^3, & w \in [w_j, w_{j+1}], \\ h^3 + 3h^2(w-w_{j+1}) + 3h(w-w_{j+1})^2 - 3(w-w_{j+1})^3, & w \in [w_{j+1}, w_{j+2}], \\ h^3 + 3h^2(w_{j+3}-w) + 3h(w_{j+3}-w)^2 - 3(w_{j+3}-w)^3, & w \in [w_{j+2}, w_{j+3}], \\ (w_{j+4}-w)^3, & w \in [w_{j+3}, w_{j+4}], \\ 0, & otherwise. \end{cases} \tag{4}$$

Note that $B_j^3(w)$, $B_{j+1}^3(w)$ and $B_{j+2}^3(w)$ are non-zero due to local support property. If we define $Q(w,t) = \sum_{j=0}^{M+1} \varphi_j(t) B_{j+2}^3(w)$ where $\varphi_j(t)$ are unknowns to be found we obtain the following approximation:

$$\begin{cases} \varphi_j(t) \approx Q(w,t) = \varphi_j(t)\left(\dfrac{1}{6}\right) + \varphi_{j+1}(t)\left(\dfrac{4}{6}\right) + \varphi_{j+2}(t)\left(\dfrac{1}{6}\right), \\ \varphi_j'(t) \approx Q'(w,t) = \varphi_j(t)\left(-\dfrac{1}{2h}\right) + \varphi_{j+2}(t)\left(\dfrac{1}{2h}\right), \\ \varphi_j''(t) \approx Q''(w,t) = \varphi_j(t)\left(\dfrac{1}{h^2}\right) + \varphi_{j+1}(t)\left(-\dfrac{2}{h^2}\right) + \varphi_{j+2}(t)\left(\dfrac{1}{h^2}\right), \end{cases} \tag{5}$$

for $j = 0, 1, 2, ..., M+1$. A distinct feature of our scheme is the treatment of the non-linear term in Eq. (1). Rather than linearizing the equation or using iterative methods, we directly approximate $\sin(\phi(s,t))$ by applying the sine function to the cubic B-spline interpolant itself, i.e., $\sin(\phi(s,t)) \approx \sin(Q(w,t))$. This ensures that the non-linearity is tackled in a manner fully consistent with the spatial discretization. Substituting the approximations from (5) for φ and its derivatives into (1) yields, for each node j, the following equation where the non-linearity is embedded within the spline representation

$$\frac{d^2\varphi_j}{dt^2} = \varphi_j(t)\left(-\frac{1}{h^2}\right) + \varphi_{j+1}(t)\left(-\frac{2}{h^2}\right) + \varphi_{j+2}(2)\left(\frac{1}{h^2}\right) - \sin(\varphi_j(t)\left(\frac{1}{6}\right) + \varphi_{j+1}\left(\frac{4}{6}\right) + \varphi_{j+2}\left(\frac{1}{6}\right)).$$

The matrix form of above equation is:

$$\frac{d^2\boldsymbol{\varphi}}{dt^2} = \boldsymbol{B}\boldsymbol{\varphi}, \tag{6}$$

where

$$\boldsymbol{B} = \begin{bmatrix} Q_0 & R_0 & S_0 & 0 & \ldots & 0 \\ 0 & Q_1 & R_1 & S_1 & \ddots & \vdots \\ \vdots & \ddots & \ddots & \ddots & \ddots & 0 \\ 0 & \ldots & Q_M & R_M & S_M & 0 \\ 0 & \ldots & 0 & Q_{M+1} & R_{M+1} & S_{M+1} \end{bmatrix}$$

and

$$\boldsymbol{\varphi} = \begin{pmatrix} \varphi_0 \\ \varphi_1 \\ \vdots \\ \vdots \\ \varphi_{M+1} \end{pmatrix},$$

with,

$$\begin{cases} Q_j = \left(-\dfrac{1}{h^2}\right) - \sin\left(\dfrac{1}{6}\right), \\ R_j = \left(-\dfrac{2}{h^2}\right) - \sin\left(\dfrac{4}{6}\right), \\ S_j = \left(\dfrac{1}{h^2}\right) - \sin\left(\dfrac{1}{6}\right), \end{cases}$$

for $j = 0, 1, 2, .., M + 1$. The system (6) of ODEs obtained is then solved using fourth order R-K method.

3 Stability Analysis

For stability analysis, we consider a linearlized version of the sine-Gordon Eq. (1). For small amplitudes, we approximate $\sin(\phi) \approx \phi$, transforming the equation into the linear Klein-Gordon equation:

$$\frac{\partial^2\varphi}{\partial t^2} = \frac{\partial^2\varphi}{\partial s^2} - \varphi, \quad s \in [\beta_1, \beta_2], \quad t > 0. \tag{7}$$

Applying our spatial discretization using cubic B-splines to Eq. (7) yields the following system of ordinary differential equations for each node j

$$\frac{d^2\varphi_j}{dt^2} = \left(\frac{1}{h^2}\varphi_j - \frac{2}{h^2}\varphi_{j+1} + \frac{1}{h^2}\varphi_{j+2}\right) - \varphi_j. \tag{8}$$

The matrix form of above semi discrete system is:

$$\frac{d^2\boldsymbol{\varphi}}{dt^2} = (\boldsymbol{D}_{xx} - \boldsymbol{I})\boldsymbol{\varphi}, \tag{9}$$

where $\boldsymbol{D}_{xx}$ is the matrix representing the cubic B-spline discretization of the second derivative, and $\boldsymbol{I}$ is the identity matrix. To analyze stability, we convert the second-order system (9) to a first-order system. Let $\boldsymbol{v} = \dfrac{d\boldsymbol{\varphi}}{dt}$. Then:

$$\frac{d}{dt}\begin{bmatrix} \boldsymbol{\varphi} \\ \boldsymbol{v} \end{bmatrix} = \begin{bmatrix} \boldsymbol{0} & \boldsymbol{I} \\ \boldsymbol{D}_{xx} - \boldsymbol{I} & \boldsymbol{0} \end{bmatrix}\begin{bmatrix} \boldsymbol{\varphi} \\ \boldsymbol{v} \end{bmatrix} = \boldsymbol{A}\begin{bmatrix} \boldsymbol{\varphi} \\ \boldsymbol{v} \end{bmatrix}. \tag{10}$$

The stability of the time integration depends on the eigenvalues of the system matrix $\boldsymbol{A}$. If λ is an eigenvalue of the spatial discretization matrix $\boldsymbol{D}_{xx}$, then the corresponding eigenvalues μ of $\boldsymbol{A}$ satisfy:

$$\mu^2 = \lambda - 1. \tag{11}$$

Since $\boldsymbol{D}_{xx}$ is a negative definite matrix for the second derivative operator, its eigenvalues are real and negative. Let $\lambda_{\min}$ be the most negative eigenvalue (largest in magnitude). Then the most restrictive eigenvalues of $\boldsymbol{A}$ are:

$$\mu_{\max} = \pm i\sqrt{|\lambda_{\min}| + 1}, \tag{12}$$

which are purely imaginary. The maximum magnitude $|\mu_{\max}|$ determines the highest frequency in our semi-discrete system.

The stability of our scheme depends critically on the spectral properties of the cubic B-spline spatial discretization matrix $\boldsymbol{D}_{xx}$. Numerical computation of the eigenvalues for our specific discretization reveals that the spectral radius scales as:

$$\rho(\boldsymbol{D}_{xx}) \approx \frac{\alpha}{h^2}$$

where $\alpha \approx 3.4$ for our formulation. This value was obtained by computing the eigenvalues of our specific cubic B-spline discretization matrix for various grid sizes and observig the consistent scaling relationship.

The stability of the fourth-order Runge-Kutta method (RK4) applied to the system (10) requires that the product $\Delta t \cdot \mu$ lies within its stability region for all eigenvalues μ of $\boldsymbol{A}$. The stability region of RK4 along the imaginary axis extends to approximately:

$$|\mu \Delta t| \lessapprox 2.83. \tag{13}$$

Applying this to our most restrictive eigenvalue $\mu_{\max}$, we obtain the stability condition:

$$\Delta t \cdot |\mu_{\max}| \lessapprox 2.83. \tag{14}$$

Substituting our eigenvalue estimate $|\mu_{\max}| \approx \sqrt{\alpha}/h$ yields:

$$\Delta t \cdot \frac{\sqrt{\alpha}}{h} \lessapprox 2.83 \quad \Rightarrow \quad \Delta t \lessapprox \frac{2.83}{\sqrt{\alpha}} h. \tag{15}$$

Using $\alpha \approx 3.4$, we obtain the practical stability condition:

$$\Delta t \lessapprox 1.53h. \tag{16}$$

4 Convergence Analysis

The convergence analysis of the proposed scheme must account for errors arising from both the spatial discretization (cubic B-splines) and the temporal integration (Runge-Kutta method). We present a comprehensive error analysis that combines theoretical foundations with empirical validation.

4.1 Spatial Convergence of the Cubic B-Spline Discretization

The core of our spatial approximation lies in the cubic B-spline interpolation. The convergence properties of cubic B-spline approximations are well-established in numerical analysis [29,30].

Theorem 1 (Cubic B-spline Approximation Error). *Let $\varphi(s) \in C^4([\beta_1, \beta_2])$ be a sufficiently smooth function and let $Q(s)$ be its cubc B-spline interpolant on a uniform partition with grid spacing h. Then, there exist constants $K_0, K_1, K_2 > 0$, independent of h, such that:*

1. ***Function Approximation:***

   $\|\varphi - Q\|_\infty \leq K_0 h^4 \|\varphi^{(4)}\|_\infty$

2. ***First Derivative:***

   $\|\varphi' - Q'\|_\infty \leq K_1 h^3 \|\varphi^{(4)}\|_\infty$

3. ***Second Derivative:***

   $\|\varphi'' - Q''\|_\infty \leq K_2 h^2 \|\varphi^{(4)}\|_\infty$

Proof: See [29] and [30] for detailed proofs based on the Taylor series expansion of the function and the properties of the B-spline basi. □

In our scheme, the critical term is the approximation of the second spatial derivative $\frac{\partial^2 \varphi}{\partial s^2}$ in Eq. (1). Theorem 1 guarantees that this discretization error is of order $O(h^2)$, provided the exact solution is sufficiently smooth.

4.2 Temporal Convergence of the Runge-Kutta Method

The method of lines reduces the sine-Gordon Eq. (1) to a system of second-order ordinary differential equations (ODEs):

$$\frac{d^2 \boldsymbol{\varphi}}{dt^2} = F(t, \boldsymbol{\varphi}),$$

where F incorporates the discretized spatial derivative and the nonlinear term. This system can be written as a larger system of first-order ODEs by introducing $\boldsymbol{v} = d\boldsymbol{\varphi}/dt$:

$$\frac{d}{dt}\begin{bmatrix} \boldsymbol{\varphi} \\ \boldsymbol{v} \end{bmatrix} = \begin{bmatrix} \boldsymbol{v} \\ F(t, \boldsymbol{\varphi}) \end{bmatrix}.$$

The standard fourth-order Runge-Kutta (RK4) method is applied to this system.

Theorem 2 (Local Truncation Error of RK4). *Suppose the right-hand side function of the ODE system is sufficiently smooth. The local truncation erro (LTE) for the RK4 method at each time step is $O(\Delta t^5)$, which implies a global error of $O(\Delta t^4)$.*

Proof: This is a classical result; see [31] for a detailed derivation using Taylor series expansion. □

4.3 Combined Error Analysis

The overall error of the fully discrete scheme is a combination of the spatial discretization error and the temporal integration error. Let $\boldsymbol{\Phi}(t)$ be the vector of the exact solution at the spatial grid points, and let $\boldsymbol{\Phi}_n$ be the numerical approximation at time t_n. Using the triangle inequality, the global error at time t_n can be decomposed as:

$$\|\boldsymbol{\Phi}(t_n) - \boldsymbol{\Phi}_n\| \leq \underbrace{\|\boldsymbol{\Phi}(t_n) - \boldsymbol{\varphi}(t_n)\|}_{\text{Spatial Error}} + \underbrace{\|\boldsymbol{\varphi}(t_n) - \boldsymbol{\Phi}_n\|}_{\text{Temporal Error}},$$

where $\boldsymbol{\varphi}(t)$ is the exact solution of the semi-discrete system of ODEs obtained after spatial discretization.

- **Spatial Error Bound:** From Theorem 1, the error in approximating the second derivative is $O(h^2)$. This error propagates through the time integration. Under stability assumptions, the error in the semi-discrete solution $\boldsymbol{\varphi}(t)$ compared to the projection of the true PDE solution $\boldsymbol{\Phi}(t)$ is also $O(h^2)$.
- **Temporal Error Bound:** From Theorem 2, the error due to the RK4 time stepping is $O(\Delta t^4)$ for the ODE system.

Therefore, the total global error is bounded by:

$$\|\boldsymbol{\Phi}(t_n) - \boldsymbol{\Phi}_n\| \leq C_1 h^2 + C_2 \Delta t^4, \tag{17}$$

where C_1 and C_2 are constants independent of h and Δt.

Remark 1 (Dominant Error Term). *The asymptotic convergence rate observed in practice will be determined by the dominant term in (17). If the spatial error dominates ($h^2 \gg \Delta t^4$), the overall convergence will be $O(h^2)$. Conversely, if the temporal error dominates ($\Delta t^4 \gg h^2$), the convergence will be $O(\Delta t^4)$. For balanced refinement, one should choose $\Delta t \sim h^{1/2}$ to equilibrate both error terms.*

4.4 Empirical Validation

The theoretical convergence rate of $O(h^2)$ for the spatial discretization is strongly supported by the empirical results presented in Section 5.

- **Example 1 (Table 3):** The L_∞ error norms for spatial refinement yield a Rate of Convergence (ROC) of approximately 1.96, which is in excellent agreement with the theoretical value of 2.
- **Example 2 (Table 6):** The ROC for spatial refinement is approximately 2.42, further validating the $O(h^2)$ theoretical prediction.
- **Example 3 (Table 9):** The ROC increases towards 2 as the grid is refined, demonstrating the asymptotic convergence behavior and the effect of non-smooth initial conditions on a coarse grid.

These empirical results confirm that the spatial error is the dominant factor in the total error for the chosen time steps, and that the cubic B-spline discretization achieves its theoretical second-order convergence.

5 Results and Discussion

The accuracy of the proposed scheme is examined and evaluated through the use of various test problems. To quantify the errors, the following errors are defined to measure the accuracy of the solutions:

- **Absolute Error:** $\|exact - approx\|$.
- L_∞**Norm:** $max\|exact - approx\|$.
- **Root Mean Square (RMS):** $\dfrac{1}{N+1}\sqrt{\sum_{j=0}^{N} \|exact - approx\|^2}$.

Rate of convergence (ROC) is analyzed by:

- **ROC:** $\dfrac{\log\left(\dfrac{E^{n_1}}{E^{n_2}}\right)}{\log\left(\dfrac{n_2}{n_1}\right)}$

where E^{n_1} and E^{n_2} are errors with n_1 and n_2, respectively.

Example 1. *Consider the sine-Gordon equation,*

$$\frac{\partial^2\varphi}{\partial t^2} = \frac{\partial^2\varphi}{\partial s^2} - \sin\varphi, \quad t > 0, \quad -2 \leq s \leq 2,$$

with the IC's:

$$\begin{cases} \varphi(s,0) = 0, \\ \varphi_t(s,0) = 4\sec(h(s)), \end{cases}$$

and the BC's:

$$\begin{cases} \varphi(-2,t) = 4\arctan(\sec(h(-2)t)), \\ \varphi(2,t) = 4\arctan(\sec(h(2)t)), 0 \leq t \leq 1. \end{cases}$$

The corresponding analytical solution is:

$$\varphi(s,t) = 4\arctan(\sec(h(s)t)).$$

Table 1 summarizes the L_∞ and RMS norms at various time steps compairing the outcomes with those obtained in [19,20,23]. Tables 2 and 3 compare the exact and approximate solutions by computing absolute errors for Example 1. Fig. 1 illustrates the exact and approximate solutions at different time steps with a step size $h = 0.01$ and $\triangle t = 0.01$. Figs. 2 and 3 depicts the absolute error in two dimensional form and space-time graph of exact and approximate solutions, respectively, for $h = 0.01$ and $\triangle t = 0.01$.

Table 1: Comparison of errors in domain $[-2,2]$ with $h = 0.01$ and $\triangle t = 0.01$ for Example 1

t	[19]		[20]		[23]		Present Scheme	
	RMS error	L_∞ norm	*RMS* error	L_∞ norm	*RMS* error	L_∞ norm	*RMS* error	L_∞ norm
0.2	1.76×10^{-5}	9.25×10^{-5}	6.55×10^{-7}	2.50×10^{-5}	2.69×10^{-7}	2.26×10^{-5}	1.49×10^{-7}	3.73×10^{-7}
0.4	1.62×10^{-4}	1.62×10^{-4}	1.15×10^{-6}	4.20×10^{-5}	1.19×10^{-6}	7.52×10^{-5}	8.65×10^{-7}	2.06×10^{-6}
0.6	1.65×10^{-4}	3.73×10^{-4}	1.55×10^{-6}	6.54×10^{-5}	2.96×10^{-6}	1.55×10^{-4}	2.21×10^{-6}	4.85×10^{-6}
0.8	2.98×10^{-4}	6.24×10^{-4}	3.92×10^{-6}	4.01×10^{-4}	5.72×10^{-6}	2.59×10^{-4}	3.88×10^{-6}	7.76×10^{-6}
1.0	4.37×10^{-4}	8.94×10^{-4}	1.56×10^{-5}	1.53×10^{-3}	9.56×10^{-6}	3.84×10^{-4}	5.55×10^{-6}	9.99×10^{-6}

Table 2: Exact solution, approximate solution and absolute error when $n = 9$, $t = 1$ and $\triangle t = 0.01$ for Example 1

s	Theoretical	Approximate	Absolute error
-1.6	1.4804	1.4730	7.33×10^{-3}
-1.2	2.0184	2.0085	9.53×10^{-3}
-0.8	2.5681	2.5651	2.97×10^{-3}
-0.4	2.9858	2.9953	9.49×10^{-3}
0.0	3.1415	3.1572	1.57×10^{-2}
0.4	2.9858	2.9953	9.49×10^{-3}
0.8	2.5681	2.5651	2.97×10^{-3}
1.2	2.0183	2.0088	9.53×10^{-3}
1.6	1.4804	1.4730	7.32×10^{-3}

Table 3: Error norm together with rate of convergence when $s \in [-2, 2]$ and $\triangle t = 0.01$ for Example 1

n	L_∞ Error	ROC	RMS Error	ROC
10	1.1775×10^{-2}	–	6.7812×10^{-3}	–
20	3.3726×10^{-3}	1.79	1.9046×10^{-3}	1.83
40	8.9427×10^{-4}	1.92	5.0573×10^{-4}	1.91
80	2.2976×10^{-4}	1.96	1.3037×10^{-4}	1.96

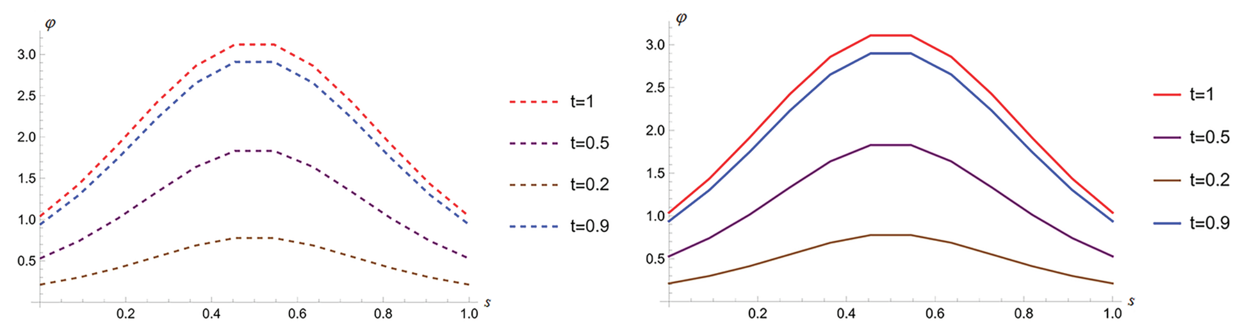

Figure 1: Time evolution of solution for Example 1 showing excellent agreement exact (right) and approximate (left) when $h = 0.01$ and $\Delta t = 0.01$

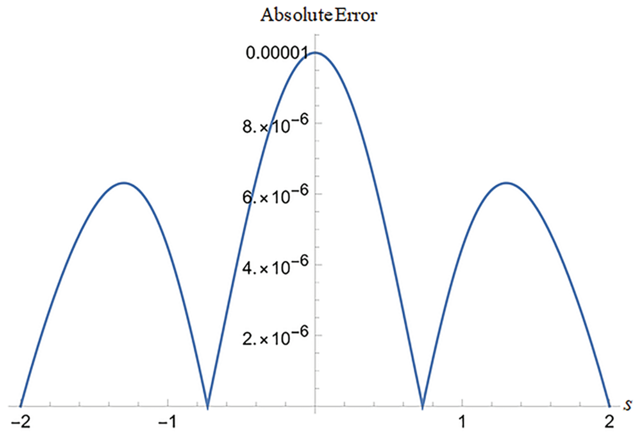

Figure 2: Absolute error distribution for Example 1 at $t = 1$ when $h = \Delta t = 0.01$. The symmetric error patters confirm the stability of our method, with errors remaining bounded throughout the computational domain

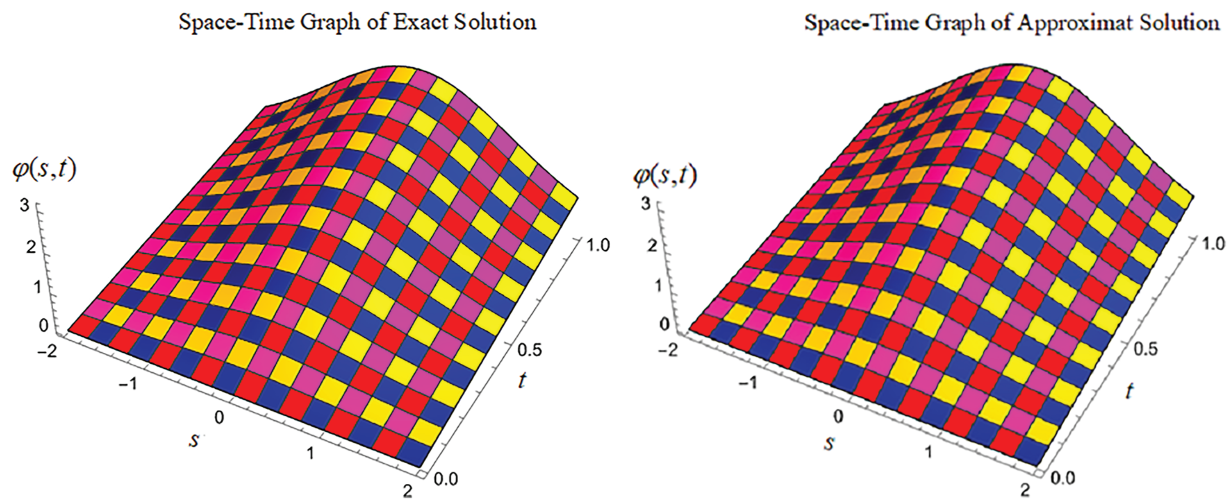

Figure 3: Space-time evolution of exact (left) and approximate (right) solutions for Example 1 over $t \in [0, 1]$ when $\Delta t = h = 0.01$

Example 2. *Consider the sine-Gordon equation,*

$$\frac{\partial^2 \varphi}{\partial t^2} = \frac{\partial^2 \varphi}{\partial s^2} - \sin \varphi, \quad t > 0, \quad -3 \leq s \leq 3,$$

having ICs,

$$\begin{cases} \varphi(s, 0) = 0, \\ \varphi_t(s, 0) = 4 \arctan e^{\tau s}, \end{cases}$$

and BCs,

$$\begin{cases} \varphi(-3,t) = 4\arctan e^{\tau(-3-\eta t)}, \\ \varphi(3,t) = 4\arctan e^{\tau(3-\eta t)}, \quad t > 0 \end{cases}$$

where, $\tau = \frac{1}{\sqrt{1-\eta^2}}$ *and* $\eta = 0.5$.

The analytical solution of the given problem is:

$\varphi(s,t) = 4\arctan e^{\tau(s-\eta t)}$.

Table 4 provides a comparison of L_∞ norm at different time stages, with the computed outcomes compared with [23]. Tables 5 and 6 present the exact solution, approximate solution and absolute errors. Fig. 4 illustrates the exact and approximate solutions at different time steps by taking $h = 0.04$ and $\triangle t = 0.0001$. Figs. 5 and 6 show the absolute error in two-dimensional form and space-time graph of exact and approximate solution at $\eta = 0.5$, $h = 0.04$ and $\triangle t = 0.0001$, respectively.

Table 4: Comparison of maximum absolute error (L_∞) with $\eta = 0.5$, $\triangle t = 0.0001$ & $h = 0.04$ for Example 2

t	[23]	Present scheme
0.25	4.90×10^{-5}	6.43×10^{-6}
0.50	7.55×10^{-5}	2.44×10^{-5}
0.75	1.43×10^{-4}	5.05×10^{-5}
1.00	2.10×10^{-4}	8.10×10^{-5}

Table 5: Exact solution, approximate solution and absolute errors when $n = 30$, $t = 0.5$ and $\triangle t = 0.0001$ for Example 2

s	Theoretical	Approximate	Absolute error
−2.8064	0.1171	0.1171	8.23243×10^{-5}
−2.6129	0.1464	0.1464	1.65775×10^{-4}
−2.4193	0.1831	0.1830	2.59479×10^{-4}
−2.2258	0.2289	0.2288	3.71248×10^{-4}
−2.0322	0.2860	0.2859	5.17694×10^{-4}
−1.8387	0.3574	0.3572	7.24952×10^{-4}
1.4516	5.3047	5.3052	2.57576×10^{-3}
1.6451	5.4951	5.4954	1.83656×10^{-3}
1.8387	5.6501	5.6502	1.27688×10^{-3}
2.2258	5.8763	5.8764	6.16663×10^{-4}
2.4193	5.9574	5.9575	4.23982×10^{-3}
2.8064	6.0746	6.0746	1.36873×10^{-4}

Table 6: Error norm together with rate of convergence when $s \in [-3, 3]$ and $\triangle t = 0.01$ for Example 2

n	L_∞ Error	*ROC*	*RMS Error*	*ROC*
10	3.5129×10^{-2}	–	1.7584×10^{-2}	–
20	9.556×10^{-3}	1.88	4.8790×10^{-3}	1.85
40	2.4261×10^{-3}	1.98	1.2049×10^{-3}	2.02
80	4.7489×10^{-4}	2.35	2.1961×10^{-4}	2.46

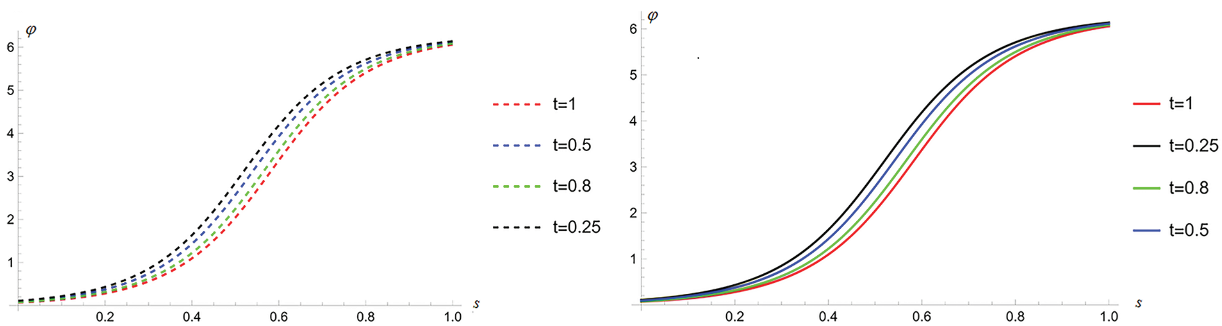

Figure 4: Time evolution of solution for Example 2 showing excellent agreement exact (right) and approximate (left) when $h = 0.04$ and $\Delta t = 0.0001$

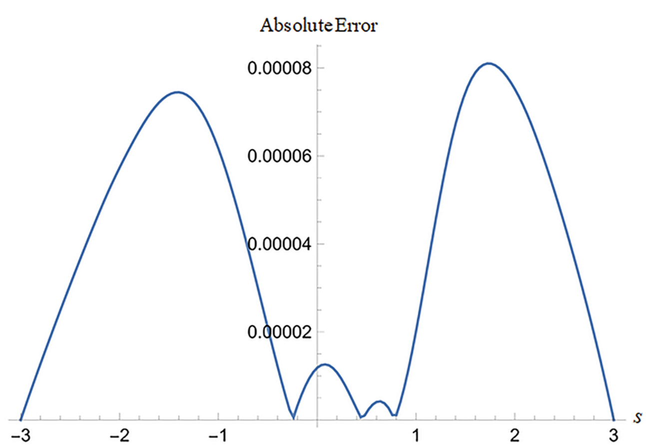

Figure 5: Absolute error distribution for Example 2 at $t = 1$ when $h = 0.04$, $\eta = 0.5$ and $\Delta t = 0.0001$. The symmetric error patters confirm the stability of our method, with errors remaining bounded throughout the computational domain

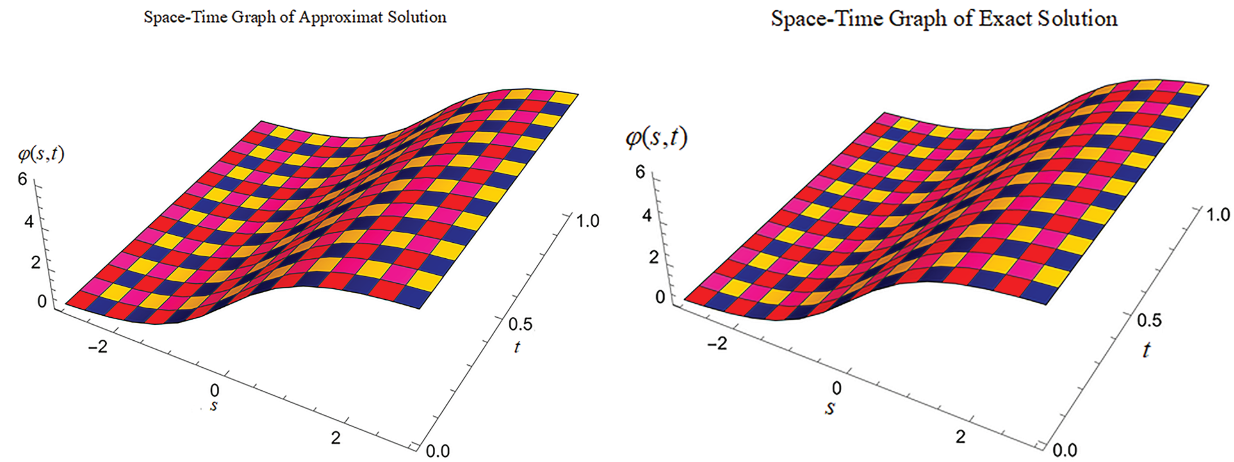

Figure 6: Space-time evolution of exact (left) and approximate (right) solutions for Example 2 over $t \in [0, 1]$ when $h = 0.04$, $\Delta t = 0.01$ and $\eta = 0.5$

Example 3. *Consider the sine-Gordon equation,*

$$\frac{\partial^2 \varphi}{\partial t^2} = \frac{\partial^2 \varphi}{\partial s^2} - \sin\varphi, \quad t > 0, \quad -10 \le s \le 10,$$

having IC's,

$$\begin{cases} \varphi(s,0) = 0, \\ \varphi_t(s,0) = 3.458\,\mathrm{sech}(0.8945s), \end{cases}$$

The exact solution of the corresponding problem is given as:

$$\varphi(s,t) = 4\tan^{-1}\left(2\sin(0.44725t)\,\mathrm{sech}(0.8945s)\right).$$

The boundary conditions are derived from theoretical solution.

The numerical results of Example 3 are calculated within the computational interval $[-10, 10]$ and the computed outcomes are compared with those from [15,24]. Table 7 presents a comparison of L_∞ norm at different time stages. Table 8 shows the exact solution, approximate solution and absolute errors. Table 9 records error norms together with convergence rates for various spatial step sizes. Fig. 7 illustrates the exact and approximate solutions at different time steps using $h = 0.01$ $\triangle t = 0.001$. Figs. 8 and 9 display the absolute error in two-dimensional form and space-time graph of exact and approximate solutions at $h = 0.01$ and $\triangle t = 0.001$ is shown, respectively.

Table 7: Comparison of maximum absolute error (L_∞) at $h = 0.01$ and $\triangle t = 0.001$ for Example 3

t	[15]	[24]	Present scheme
1	0.98816×10^{-3}	1.474×10^{-3}	6.14×10^{-5}
10	0.16291×10^{-2}	9.215×10^{-3}	2.96×10^{-4}
20	0.10379×10^{-1}	3.038×10^{-1}	5.42×10^{-4}

Table 8: Exact solution, approximate solution and absolute error when $n = 9$, $t = 1$ and $\triangle t = 0.001$ for Example 3

s	Theoretical	Approximate	Absolute error
-8	0.0054	0.0049	4.0499×10^{-4}
-6	0.0323	0.0298	2.4233×10^{-3}
-4	0.1929	0.1783	1.4627×10^{-2}
-2	1.0967	1.0146	8.2104×10^{-2}
0	2.8525	3.0698	2.1735×10^{-2}
2	1.0967	1.0146	8.2104×10^{-2}
4	0.1929	0.1783	1.4627×10^{-3}
6	0.3230	0.0298	2.4233×10^{-4}
8	0.0053	0.0049	4.0449×10^{-3}

Table 9: Error norm together with rate of convergence when $s \in [-10, 10]$ and $\triangle t = 0.01$ for Example 3

n	L_∞ Error	ROC	RMS Error	ROC
10	3.7916×10^{-2}	–	1.7396×10^{-2}	–
20	3.2401×10^{-2}	0.23	1.4665×10^{-2}	0.25
40	1.4815×10^{-2}	1.13	4.3914×10^{-3}	1.74
80	4.1947×10^{-3}	1.82	1.1366×10^{-3}	1.95

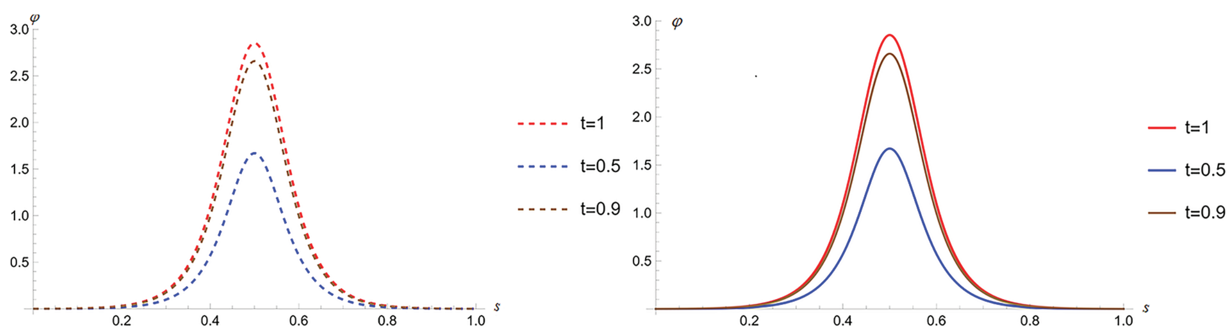

Figure 7: Time evolution of solution for Example 3 showing excellent agreement exact (right) and approximate (left) when $h = 0.01$ and $\Delta t = 0.001$

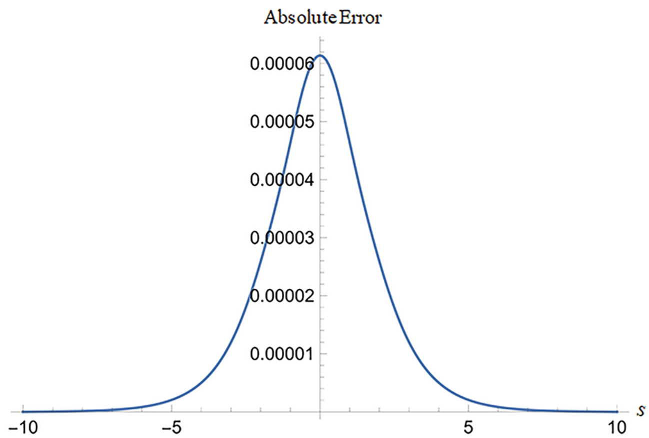

Figure 8: Absolute error distribution for Example 3 at $t = 1$ when $h = 0.01$ and $\Delta t = 0.0001$. The symmetric error patters confirm the stability of our method, with errors remaining bounded throughout the computational domain

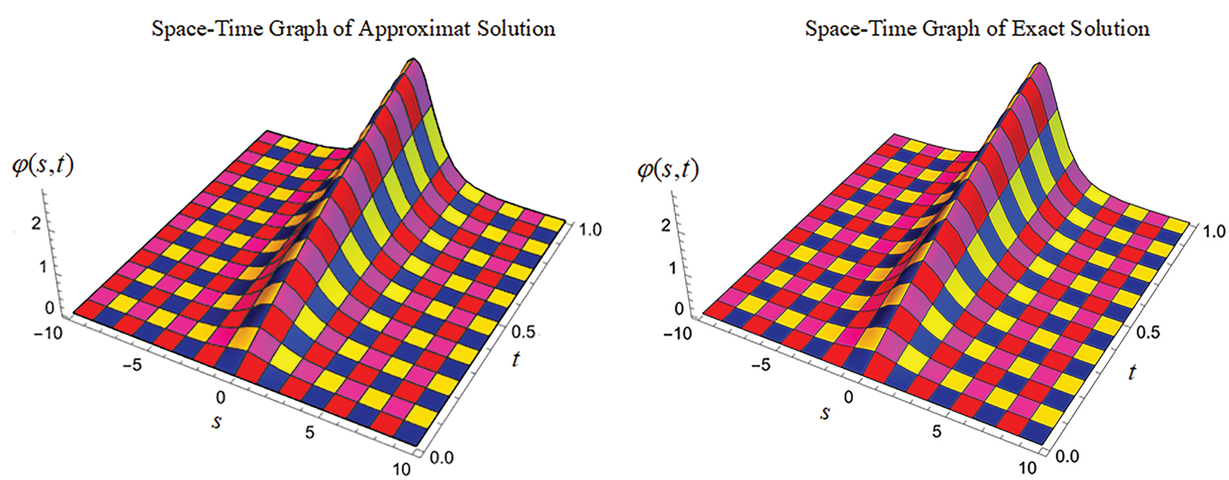

Figure 9: Space-time evolution of exact (left) and approximate (right) solutions for Example 3 over $t \in [0, 1]$ when $h = 0.01$, $\Delta t = 0.001$

6 Concluding Remarks

This article has outlined a numerical scheme for the sine-Gordon equation using the method of lines together with space discretization using cubic B-splines. The most original part of this contribution is in the specific combination of these techniques and its implemented efficiency. Our technique, as opposed to the other spline based approaches, takes advantage of the thoroughly studied characteristics of cubic B-splines. Moreover, unlike other cubic B-spline methods like the DQM technique, our scheme takes advantage of a simple RK4 solver with high precision and computational efficiency without requiring more sophisticated time-stepping schemes. The numerical solution confirms that this specific combination is a robust substitute for existing spline-based solutions. Furthermore, the utilization of cubic B-spline interpolation within the method of lines framework offers an optimistic numerical approach. The spatial derivative is approximated using cubic

B-splins following the discretization of the spatial domain and approximating the spatial derivative with cubic B-splines, we have demonstrated high accuracy and stability in our numerical simulations. The resulting system of ordinary differential equations is solved reliably using the Runge-Kutta method. Our method exhibits computational efficiency and accuracy when compared to existing approaches, making it better tool for studying the dynamics and behavior of systems governed by the sine-Gordon equation. Further research could explore the extension of this method to higher dimensions and its applications to more complex systems in physics and engineering.

Acknowledgement: We acknowledge the support of the Deanship of Scientific Research, Vice Presidency for Graduate Studies and Scientific Research, King Faisal University, Saudi Arabia.

Funding Statement: This work was supported by the Deanship of Scientific Research, Vice Presidency for Graduate Studies and Scientific Research, King Faisal University, Saudi Arabia [Grant No. KFU253959].

Author Contributions: The authors confirm contribution to the paper as follows: Conceptualization, Muhammad Yaseeen and Irsa Ashraf; methodology, Salma Trabelsi and Irsa Ashraf; software, Muhammad Yaseeen; validation, Irsa Ashraf and Marwa Balti; formal analysis, Salma Trabelsi and Marwa Balti; investigation, Irsa Ashraf, Muhammad Yaseeen and Salma Trabelsi; writing—original draft preparation, Irsa Ashraf and Muhammad Yaseeen; data curation, Muhammad Yaseeen, Salma Trabelsi and Marwa Balti; visualization, Muhammad Yaseeen and Marwa Balti; funding acquisition, Salma Trabelsi and Marwa Balti. All authors reviewed the results and approved the final version of the manuscript.

Availability of Data and Materials: Not applicable.

Ethics Approval: Not applicable.

Conflicts of Interest: The authors declare no conflicts of interest to report regarding the present study.

References

1. Dehghan M, Shokri A. Numerical solution of the non-linear Klein-Gordon equation using radial basis functions. Int J Appl Comput Math. 2009;230(2):400–10. doi:10.1016/j.cam.2008.12.011.
2. Jokela N, Keski-Vakkuri E, Majumder J. Timelike boundary sine-Gordon theory and two-component plasma. Phys Rev D. 2008;77(2):023523. doi:10.1103/PhysRevD.77.023523.
3. Novkoski F, Falcon E, Pham CT. A numerical direct scattering method for the periodic sine-Gordon equation. European Physical Journal Plus. 2023;138:1146. doi:10.1140/epjp/s13360-023-04706-7.
4. Tamsir M, Meetei MZ, Dhiman N. Numerical treatment of the Sine-Gordon equations via a new DQM based on cubic unified and extended trigonometric B-spline functions. Wave Motion. 2024;131(4):103409. doi:10.1016/j.wavemoti.2024.103409.
5. Chu YM, Fahim MRA, Kundu PR, Islam ME, Akbar MA, Inc M. Extension of the sine-Gordon expansion scheme and parametric effect analysis for higher-dimensional nonlinear evolution equations. J King Saud Univ Sci. 2021;33(6):101515. doi:10.1016/j.jksus.2021.101515.
6. Wang G, Yang K, Gu H, Guan F, Kara AH. A (2+1)-dimensional sine-Gordon and sinh-Gordon equations with symmetries and kink wave solutions. Nucl Phys B. 2020;953:114956. doi:10.1016/j.nuclphysb.2020.114956.

7. K S, Veeresha P, Prakasha DG, Malagi NS, Ramane HS, Pise KS. Novel approaches for nonlinear Sine-Gordon equations using two efficient techniques. Int J Model Simul. 2024.
8. Li H, Chen X. Numerical method and analysis for the coupled Sine-Gordon equations on unbounded domains. Numer Methods Partial Differ Equ. 2024;41(4):e70015. doi:10.1002/num.70015.
9. Mohebbi A, Dehghan M. High-order solution of one-dimensional sine-Gordon equation using compact finite difference and Dirkn method. Math Comput Model Dyn Syst. 2010;51(5–6):537–49. doi:10.1016/j.mcm.2009.11.015.
10. Uddin M, Hussain A, Haq S, Ali A. RBF meshless method of lines for the numerical solution of nonlinear sine-Gordon equation. Eng Phys Sci. 2014;11(4):349–60.
11. Savović S, Ivanović M, Drljaća B, Simović A. Numerical solution of the sine-Gordon equation by novel physics-informed neural networks and two different finite difference methods. Axioms. 2024;13(12):872. doi:10.3390/axioms13120872.
12. Wei GW. Discrete singular convolution for the sine-Gordon equation. Physica D: Nonlin Phenom. 2000;137(3–4):247–59. doi:10.1016/s0167-2789(99)00186-4.
13. Batiha B, Noorani MSM, Hashim I. Numerical solution of sine-Gordon equation by variational iteration method. Phys Lett A. 2007;370(5–6):437–40. doi:10.1016/j.physleta.2007.05.087.
14. Zheng C. Numerical solution to the sine-Gordon equation defined on the whole real axis. SIAM J Sci Comput. 2007;29(6):2494–506. doi:10.1137/050640643.
15. Bratsos AG. A fourth order numerical scheme for the one-dimensional sine-Gordon equation. Int J Comput Mathem. 2008;85(7):1083–95. doi:10.1080/00207160701473939.
16. Dehghan M, Shokri A. A numerical method for one-dimensional nonlinear sine-Gordon equation using collocation and radial basis functions. Numer Methods Partial Differ Equ. 2008;24(2):687–98. doi:10.1002/num.20289.
17. Dehghan M, Mirzaei D. The boundary integral equation approach for numerical solution of the one-dimensional sine-Gordon equation. Numer Methods Partial Differ Equ. 2008;24(6):1405–15. doi:10.1002/num.20325.
18. Rashidinia J, Mohammadi R. Tension spline solution of non-linear sine-Gordon equation. Numer Algorithms. 2011;56(1):129–42. doi:10.1007/s11075-010-9377-x.
19. Ma L-M, Wang Z-M. A numerical method for one-dimensional non-linear sine-Gordon equation using multi-quadric quasi-interpolation. Chin Phys B. 2009;18(8):3099–101.
20. Jiang ZW, Wang RH. Numerical solution of one-dimensional sine-Gordon equation using high accuracy multiquadric quasi-interpolation. Appl Math Comput. 2012;218(14):7711–6. doi:10.1016/j.amc.2011.12.095.
21. Khan A, Junaid M, Khan I, Ali F, Shah K, Khan D. Application of homotopy analysis natural transform method to the solution of non-linear partial differential equations. Sci Int. 2017;29(2):297–303.
22. Yaseen M, Samraiz M. The modified new iterative method for solving linear and non-linear Klein-Gordon equation. Appl Math Lett. 2012;6(12):2979–87.
23. Mittal RC, Bhatia R. Numerical solution of non-linear sine-Gordon equation by modified cubic B-spline collocation method. Int J Partial Differ Equ. 2014;8(1):8. doi:10.1155/2014/343497.
24. Uddin M, Haq S, Qasim G. A meshfree approach for the numerical solution of nonlinear sine-Gordon equation. Int Math Forum. 2012;7(21–24):1179–86.
25. Raslan KR, Soliman AA, Ali KK, Gaber M, Almhdy SR. Numerical solution for the Sin-Gordon equation using the finite difference method and the non-standard finite difference method. Appl Mathem Inform Sci. 2023;17(2):253–60. doi:10.24297/jam.v15i0.7981.
26. Vivas-Cortez M, Huntul MJ, Khalid M, Shafiq M, Abbas M, Iqbal MK. Application of an extended cubic B-spline to find the numerical solution of the generalized nonlinear time-fractional Klein-Gordon equation in mathematical physics. Computation. 2024;12(4):80. doi:10.3390/computation12040080.

27. Deresse AT, Dufera TT. A deep learning approach: physics-informed neural networks for solving the 2D nonlinear Sine-Gordon equation. Res Appl Mathem. 2025;25(3):100532. doi:10.1016/j.rinam.2024.100532.
28. Deresse AT, Dufera TT. Exploring physics-informed neural networks for the generalizednonlinear sine-gordon equation. Appl Comput Intell Soft Comput. 2024;2024:22. doi:10.1155/2024/3328977.
29. de Boor C. A practical guide to splines. Berlin/Heidelberg, Germany: Springer-Verlag; 2001.
30. Schumaker LL. Spline functions: basic theory. Cambridge, UK: Cambridge University Press; 2007.
31. Hairer E, Nørsett SP, Wanner G. Solving ordinary differential equations I: nonstiff problems. Berlin/Heidelberg, Germany: Springer-Verlag; 1993.